

Measurement of eye aberrations in a speckle field

A V Larichev, P V Ivanov, I G Iroshnikov, V I Shmal'gauzen

Abstract. The influence of speckles on the performance of a Shark–Hartmann wavefront sensor is investigated in the eye aberration studies. The dependence of the phase distortion measurement error on the characteristic speckle size is determined experimentally. Scanning of the reference source was used to suppress the speckle structure of the laser beam scattered by the retina. The technique developed by us made it possible to study the time dependence of the human eye aberrations with a resolution of 30 ms.

Keywords: eye aberrations, Shark–Hartmann wavefront sensor, speckles.

1. Introduction

The speckle field formed upon scattering of a laser beam in a random medium is often one of the main factors restricting the performance of wavefront sensors [1–3]. The problems of investigating the effect of speckles on the performance of wavefront sensors can be divided into two main groups. The first group involves the evaluation of the phase of the speckle field itself, while the second concerns the determination of large-scale phase distortions in the presence of speckles. Such a problem arises, for example, during the measurement of human eye aberrations using a coherent illumination. For this purpose, the laser radiation is focused on the retina, forming a virtual reference source. The scattered radiation emerging from the eye is directed on the wavefront sensor. The microstructure of the retina (the mosaic formed by the photoreceptors, microvessels and capillaries) forms a speckle field, which significantly lowers the precision with which the aberrations are determined. In problems of this kind, the random modulation of the phase and intensity of the speckle field can be treated as a disturbance while determining large-scale phase distortions.

A V Larichev International Teaching and Research Laser Center, M V Lomonosov Moscow State University, Vorob'evy gory, 119899 Moscow, Russia; e-mail: larichev@iname.ru;

P V Ivanov Institute of Laser and Information Technologies, Russian Academy of Sciences, Svyatozerskaya ul. 1, 140700 Shatura, Moscow Oblast, Russia; e-mail: ivpavel@iname.ru;

I G Iroshnikov, V I Shmal'gauzen Department of Physics, M V Lomonosov Moscow State University, Vorob'evy gory, 119899 Moscow, Russia

Received 24 July 2001

Kvantovaya Elektronika 31 (12) 1108–1112 (2001)

This paper aims at an experimental study of the influence of a speckle field on the precision of human eye aberration measurements with the help of a Shark–Hartmann wavefront sensor [4].

2. Experimental setup

It was shown in papers [5–8] that the amplitude of human eye aberrations usually decreases sharply with increasing their order. This allows the use of Shark–Hartmann wavefront sensors for determining these aberrations.

In order to determine the aberrations of the eye and to study the effect of speckles on the wavefront sensors, an experimental setup shown in Fig. 1 was constructed. A diode laser beam (1) ($\lambda = 0.67 \mu\text{m}$) passes through a diaphragm (not shown in the figure) of diameter 0.8 mm. First, the diaphragm reduces the radiation power incident on the eye and second, it decreases the phase distortions acquired by the beam before its incidence on the retina, which makes it possible to satisfy the single-pass measurement conditions. After passing through the polarisation beamsplitter cube (2), confocally arranged lenses (3, 5, 8)

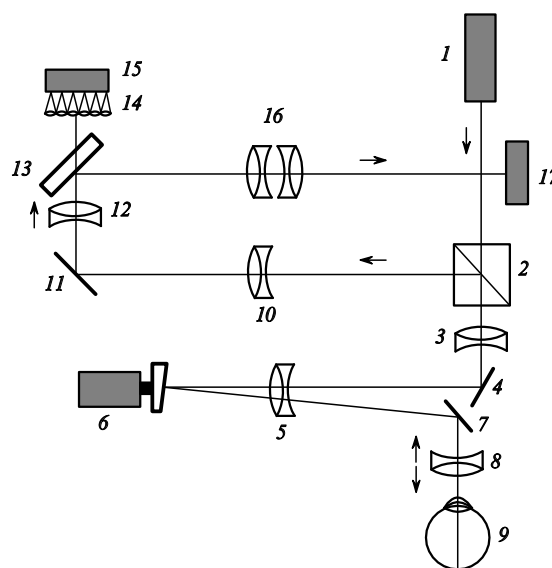


Figure 1. Schematic diagram of the experimental setup: (1) laser; (2) beamsplitter cube; (3, 5, 8, 10, 12, 16) lenses; (4, 7, 11) mirrors; (6) scanner mirror; (9) eye; (13) beamsplitter; (14) Shark–Hartmann wavefront sensor; (15, 17) CCD cameras.

and mirrors (4, 6, 7), the beam falls on the eye (9) and is focused on the retina, forming a reference light source. The radiation power incident on the eye is 30 μW , which is an order of magnitude lower than the maximum admissible power level [9, 10].

Measurement of the eye aberrations consists in the measurement of large-scale phase distortions in the plane of the pupil of the eye. The radiation emerging from the eye propagates in the reverse direction through lenses (8, 5, 3), is reflected from mirrors (7, 6, 4), and is incident on the polarisation cube (2). The cube is set in such a way that it eliminates polarised flare spots and directs only the depolarised part of the radiation scattered by the retina to the sensor. After this, light passes through confocal lenses (10, 12), is reflected by the mirror (11), and falls on the lens array (14) of the Shark–Hartmann wavefront sensor, which is placed in a plane optically conjugate to the plane of the pupil of the eye.

Each lens of the array (subaperture) has a size $A_{\text{sub}} = 0.5$ mm and a focal length $F_{\text{sub}} = 25$ mm. For a pupil diameter equal to 6 mm, the radiation emerging from the eye illuminates about 80 subapertures of the array. The lenses of the sensor divide the wavefront being studied, forming an array of spots (Hartmannogram) in the focal plane. Each spot of the Hartmannogram is an image of the reference source at the retina. The obtained Hartmannogram is recorded with a CCD camera (15) located in the focal plane of the lens raster, and is stored in the computer memory with a frequency of 30 frames s^{-1} and a resolution of 640×480 pixels. The processing time for a Hartmannogram is 8 ms. The wavefront is reconstructed by the method of least squares [4] in the form of an expansion in 36 Zernicke polynomials [11].

The light deviated by the beamsplitter (13) passes through the lens (16) and is recorded by a second CCD camera (17) located in a plane optically conjugate to the plane of the pupil of the eye. This camera is used for observing the speckle field.

The speckle structure of the field scattered by the retina lowers the accuracy of measurement of aberrations. It was shown in paper [7] that owing to the eye movements, the speckles can be suppressed considerably due to time integration. However, such a regime of the system operation does not allow the measurement of aberrations of the eye at a high speed. In our system, a different method of speckle suppression, namely, the scanning of the position of the reference source, is used. For this purpose, a mirror (6) was fixed to the axis of rotation of an electric motor at a small angle equal to 0.5° . As the mirror rotates, the reflected laser beam describes a cone, resulting in a displacement of the reference source on the retina and, consequently, in a change in the speckle structure.

In the general case, the wavefront tilt caused by the scanner mirror may result in an undesirable displacement of the Hartmannogram spots. To eliminate this effect, the optical diagram is organised in such a way that the beam leaving the eye is reflected again from the scanner mirror so that the tilts caused by this mirror are compensated. In our case, the reference source describes on the retina a circle of diameter 150 μm , and the Hartmannogram spots remain stationary. For a rotation speed of 50 cycles s^{-1} of the electric motor, the characteristic time of speckle variation was much shorter than the integration time of the CCD camera (30 ms), and the speckles were effectively averaged.

3. Method of Hartmannograms processing

When a beam with a distorted wavefront is supplied at the input of a sensor, each spot in the Hartmannogram is displaced relative to the subaperture axis. In the geometrical optics approximation, the local tilts φ_x and φ_y of the wavefront within a given subaperture are proportional to the displacements Δx and Δy of the spot: $\varphi_x = \Delta x/F_{\text{sub}}$, $\varphi_y = \Delta y/F_{\text{sub}}$.

In actual practice, the displacements of the spots are determined relative to the reference Hartmannogram corresponding to a plane wavefront. Two algorithms for determining the positions of the spots have received wide recognition. These are the centre-of-mass method and the method based on the approximation of the intensity distribution at a spot by a second-order surface [12]. In the centre-of-mass technique, the coordinates x and y of the spot in a subaperture are defined by the formulas

$$x = \frac{\sum_{i=1}^m \sum_{j=1}^n I_{ij} x_i}{\sum_{i=1}^m \sum_{j=1}^n I_{ij}}, \quad y = \frac{\sum_{i=1}^m \sum_{j=1}^n I_{ij} y_j}{\sum_{i=1}^m \sum_{j=1}^n I_{ij}}, \quad (1)$$

where the summation is carried out over the area of the Hartmannogram covered by one subaperture of the lens raster, and I_{ij} is the intensity at a point with coordinates x_j , y_j . In the absence of a noise, the displacement of the centre of mass of a spot is proportional to the wavefront tilt averaged over the subaperture.

In the second algorithm, the spot intensity profile is approximated by the surface

$$S(x, y) = ax^2 + by^2 + cxy + dx + ey + g, \quad (2)$$

where a , b , c , d , e and g are unknown parameters which are determined from the condition of minimum mean-square deviation. The coordinates of the maximum of the function $S(x, y)$ are taken as the true position of the spot centre.

In the general case, the coordinates of the spot centres determined with the help of these algorithms do not coincide. The second method is less sensitive to noise, but it is applicable only if the intensity distribution in the spot does not have clearly manifested local extrema. In the presence of speckles, the shape of the spots is no longer symmetric and the spots become irregular in shape. In this case, the centre-of-mass technique is preferable. In our programme for determining the spot positions, both algorithms were used. In the case of spots with monotonic intensity distribution close to the diffractionally limited distribution, we used the second-order surface approximation, which describes the spot position with a high degree of precision. In the other case, the centre-of-mass algorithm was used.

4. Calibration of the system

The optical diagram shown in Fig. 1 maps the plane of the eye pupil onto the lens raster plane with a certain magnification q , which leads to a change in the local tilts of the wavefront. Thus, in order to determine the wavefront in the plane of the eye pupil, the local tilts measured in the sensor plane should be divided by q . In the general case,

knowing the focal lengths of the lenses and their position, we can calculate the magnification of the system. However, in actual practice it is necessary to take into account the imperfection of the optical system, the production tolerances for the focal lengths of lenses and the mounting errors for them. This leads to a correcting calibration factor δ , which has to be determined experimentally.

To determine the correction δ , we used the model of the eye consisting of a lens with focal length $f = 25$ mm and a scatterer (fibre glass washer with a fibre diameter $6 \mu\text{m}$) imitating the eye retina. A laser beam was focused by the lens at the front plane face of the washer. After this, light propagated along the fibres, was reflected at the back face of the washer, travelled in the backward direction, and formed a reference source at the front face of the washer. The phases of the radiation emerging from different fibres are virtually not correlated. In order to reduce the power of the radiation emerging from the model of the eye, a filter was installed in front of the washer. The fibre glass washer was fastened on a micrometer translation stage that allowed its displacement with an error of $10 \mu\text{m}$. Fig. 2 shows the intensity distributions in the plane of the pupil in the eye model, as well as the Hartmannogram obtained with and without the scanner. One can see that scanner allows an effective suppression of the speckle structure and improves the quality of the Hartmannogram.

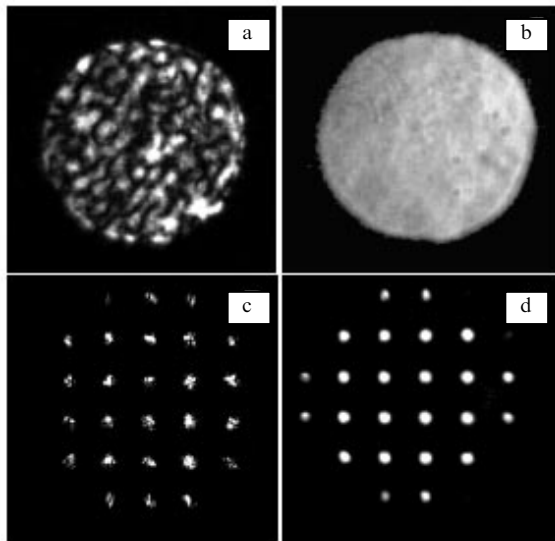


Figure 2. Intensity distributions in the plane of the pupil of the eye model (a, b) and Hartmannograms (c, d) without (a, c) and with (b, d) scanner.

The calibration of the system was done with the scanner on. To obtain the reference Hartmannogram, the glass fibre washer was mounted strictly in the focal plane of the lens. In this case, the wavefront in the plane of the eye was flat. Note that light propagates over the entire optical track during recording of the reference Hartmannogram, and the initial plane beam acquires phase distortions caused by the aberrations of the system. Since the displacements of the spots were determined relative to the reference Hartmannogram, subsequent measurements were insensitive to the aberrations of the system itself.

The defocusing D of the eye model in diopters is defined by the expression

$$D = \frac{\Delta_{\text{rel}}}{(1 + \Delta_{\text{rel}})}, \quad \Delta_{\text{rel}} = \frac{\Delta}{f}, \quad (3)$$

where Δ is the displacement of the front face of the glass fibre washer from the focal plane of the lens. To calibrate the system, the dependence of D on the separation between the lens and the scatterer was determined both experimentally and theoretically [using formula (3)]. The calibration coefficient δ was chosen so that the difference between the experimental and theoretical curves was minimum. The defocusing measured on our setup differed from the theoretical value by not more than 2%. The standard deviation of the experimental values (each point was obtained as a result of averaging over 20 realisations) did not exceed 0.002 diopters.

5. Influence of the speckle field on the accuracy of wavefront reconstruction

The speckle field statistics depends on the diameter of the illuminated spot at the scatterer. For example, the speckle size is the largest when the front face of the glass fibre washer coincides with the focal plane of the lens. A displacement of the lens along the optical axis leads to a change in the size of the illuminated spot and hence to a change in the speckle size.

The correlation radius r_{cor} of the speckle field is determined from the $1/e$ level of the structural intensity function:

$$G(\Delta r) = \langle [I(r + \Delta r) - I(r)]^2 \rangle,$$

where $I(r)$ is the intensity distribution in the speckle field; Δr is the transverse shift, and the angle brackets indicate space averaging. In the case of a statistically uniform field, the space averaging is equivalent to averaging over an ensemble of various realisations of speckles. This property was used for calculating the structural function and the error in reconstructing the wavefront.

The glass fibre washer in the experiments was displaced in a plane perpendicular to the optical axis. The statistics of various realisations of the speckle field was compiled in this manner. The characteristic scale of speckles, determined by the separation between the lens and the scatterer remained unchanged in this case. Wavefront measurements for various realisations of the speckle field were carried out without the scanner. The set of Zernicke coefficients determined in this way was used to determine their mean square deviation $\sigma_i = \langle (a_i - \langle a_i \rangle)^2 \rangle$ (a_i is the i th Zernicke coefficient) characterising the phase reconstruction error associated with the presence of speckles. After this, the glass fibre washer was displaced longitudinally. The speckle size varied in this case, and the procedure for determining the error was repeated.

Fig. 3 shows the intensity distributions in a speckle field and the Hartmannograms for two different ratios of the correlation radius to the size of the subaperture: $r_{\text{cor}}/A_{\text{sub}} = 0.3$ (large speckles, Figs 3a and c) and $r_{\text{cor}}/A_{\text{sub}} = 0.07$ (fine speckles, Figs 3b and d), as well as the structural intensity modulation functions (Fig. 3e). It should be noted that the visual size of the speckles is several times larger than the correlation radius r_{cor} .

One can see from Fig. 3d that the Hartmannogram spots are split when the characteristic size of the speckles becomes

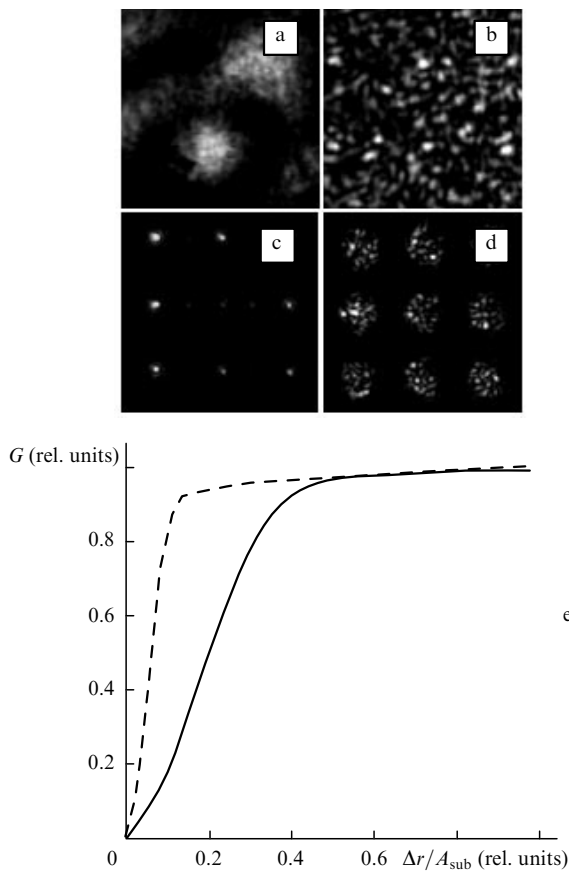


Figure 3. Intensity distributions in the speckle field (a, b) and Hartmannograms (c, d) for large (a, c) and small (b, d) speckles, as well as the intensity modulation structural functions G corresponding to large (solid line) and small (dashed line) speckles.

smaller than the subaperture size, and this leads to the emergence of additional extrema. In this case, we should use the centre-of-mass technique, which in the absence of noise gives a wavefront tilt averaged over the subaperture, irrespective of the size of phase inhomogeneities. If the characteristic size of the speckles exceeds the subaperture size, the intensity distribution inside each spot tends to the diffraction-limited distribution. However, one can see from Fig. 3c that some of the spots corresponding to the subapertures, on which dark speckles are incident, have a low intensity compared with the noise. The accuracy with which the centres of such spots are located is not very high and, therefore, they should be discarded while processing the Hartmannogram. This leads to a decrease in the accuracy of phase evaluation.

Fig. 4 shows the dependences of the mean error σ in determining the Zernicke coefficients of various orders (in the present case, the order of the polynomial is determined by the highest power of its radial argument r) (Fig. 4a) and the relative error $\sigma_{\text{rel}} = \sigma_3/a_3$ in determining the defocusing, on the ratio $r_{\text{cor}}/A_{\text{sub}}$ of the correlation radius of the speckle field to the subaperture size of the Shark-Hartmann sensor (Fig. 4b). The experimental dependences were averaged over 20 different realisations of the speckle field. One can see from Fig. 4 that as the speckle size decreases, the error σ increases for polynomials of each order. This is due to a lower accuracy with which the position of the spots is determined. For large speckles, the error in the wavefront reconstruction mainly comes from the random smooth phase distortions of the speckle field itself. In addition,

the increased error is associated with a decrease in the number of spots whose intensity is sufficient to allow their processing. One can see from Fig. 4 that in the range of variation of the ratio $r_{\text{cor}}/A_{\text{sub}} = 0.2 - 0.7$, the error in determining the Zernicke coefficients varies insignificantly, and does not exceed $0.05 \mu\text{m}$, while the relative error in determining the defocusing is no more than 10%.

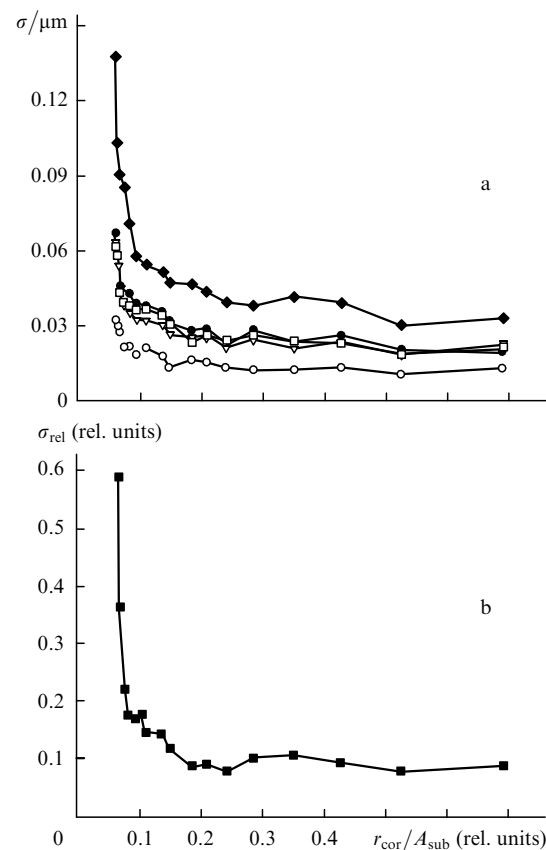


Figure 4. (a) Dependences of the mean statistical deviation of the Zernicke coefficient σ of the first (\blacklozenge), second (\bullet), third (∇), fourth (\square) and fifth (\circ) order and (b) the relative error in determining the defocusing σ_{rel} on the ratio $r_{\text{cor}}/A_{\text{sub}}$ of the correlation radius of the speckle field to the size of the subaperture.

6. Measurements of the human eye aberrations

We measured the real human eye aberrations using the scan system. In this case, the wavefront was recorded at a frequency of 30 Hz. Note that the scan not only allows a suppression of the speckle structure, but also decreases the average intensity of laser radiation at the retina of the eye by a factor of about 30.

Unlike the model eye, the real human eye may display time fluctuations of the aberrations associated with accommodation and microscopic movements (saccades) of the eye, etc. We observed the variation in the eye aberrations with time. Fig. 5 shows the amplitudes a_i of the aberrations, measured for 20 s. The eye pupil was dilated to the size 6 mm by using 2.5% Phenylephrine Hydrochloride eye drops that do not paralyse accommodation. One can see from Fig. 5 that the main aberrations in the eye under investigation are defocusing and astigmatism. A sharp increase in the aberration amplitude between sixteenth and eighteenth seconds is caused by the appearance of tears.

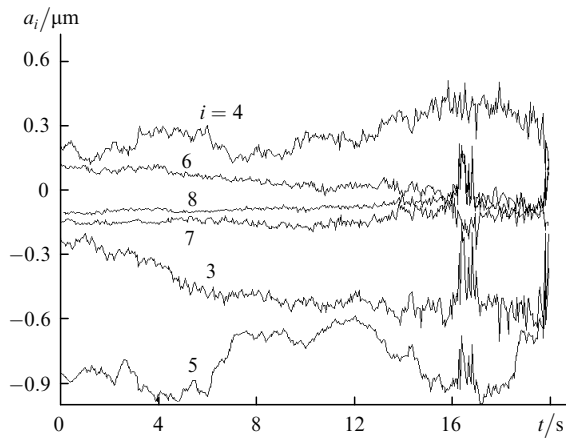


Figure 5. Time dependences of the amplitude a_i of defocusing ($i = 3$), astigmatism ($i = 4, 5$ in x, y), coma ($i = 6, 7$ in x, y), and spherical aberration ($i = 8$).

Fig. 6 shows the normalised spectral density $S(\nu)$ of the aberration fluctuations averaged over the first ten Zernicke coefficients, as well as their linear approximation. In the frequency range below 5 Hz, the aberration spectrum decays at the rate of about 4 dB octave⁻¹. For higher frequencies, the spectral density of the eye aberration fluctuations is comparable with the instrumental noise.

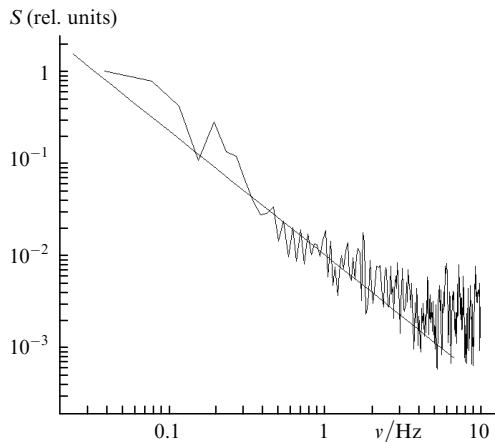


Figure 6. Normalised spectral fluctuation density of aberration fluctuations, averaged over the first ten aberrations, and its linear approximation by the function $\lg S = -2.0 - 1.35\nu$.

7. Discussion of results

Studies of the effect of speckles on the performance of the Shark–Hartmann wavefront sensor have revealed that the error in phase restoration is caused by a deterioration of the quality of the Hartmannogram being recorded. If the speckle size exceeds the size of the sensor subaperture, the main contribution to the error in determining the phase comes from the random phase modulation of the speckle field itself. In addition, some low-intensity spots in the Hartmannogram have to be excluded during signal processing. In this case, the use of a CCD camera with a broad dynamic range will increase the number of spots available for analysis. For small speckles, the Hartmannogram spots are split, and this also increases the error in determining

their centres. The centre-of-mass technique makes it possible to average the small-scale structure in the subaperture and to separate the smoothly varying local tilt of the wavefront associated with the eye aberration.

For a known speckle-field statistics, an appropriate choice of the sensor subaperture size helps minimise the error in determining the large-scale phase distortions. Measurements on the model eye show that in the range of variation of the ratio $r_{\text{cor}}/A_{\text{sub}} = 0.2 - 0.7$, the error in determining the Zernicke coefficients using the centre-of-mass algorithm does not vary significantly, and does not exceed $\lambda/15$.

Measurements on real human eye have shown that the speckle structure formed upon scattering of the laser radiation by the retina is the main factor restricting the precision of wavefront reconstruction. Scanning of the reference source over the retina efficiently suppresses the speckle structure without affecting the speed of the system. It should be noted that the reference source must not leave the isoplanatism region of the optical system of the eye during scanning.

The experiments have revealed a strong dependence of the eye aberration on time. We believe that this factor must be taken into account during corrective surgery of the eye. The medical conclusions should probably be based on the time-averaged eye aberrations.

Acknowledgements. This work was supported by the NATO programme ‘Science for Peace’ (Project Code SFP 974292). The authors thank K S Nesteruk for his help in developing the software and A Yu Resnyanskii for his help in the building of the apparatus for measurements.

References

1. Strohbehn J W *Laser Beam Propagation in the Atmosphere* (Berlin: Springer-Verlag, 1978).
2. Vorontsov M A, Shmal'gauzen V I *Printsipy adaptivnoi optiki* (Principles of Adaptive Optics), (Moscow: Nauka 1985).
3. Larichev A V, Iroshnikov N G, Nikolaev I P, Nestereouk K S, Kudryashov A V *Proc. SPIE Int. Soc. Opt. Eng.* **4162** 158 (2000).
4. Vorontsov M A, Koryabin A V, Shmal'gauzen V I *Upravlyaemye opticheskie sistemy* (Controlled Optical Systems) (Moscow: Nauka 1988).
5. Liang J, Williams D R *J. Opt. Soc. Am. A* **14** 2873 (1997).
6. Liang J, Williams D R, Miller D T *J. Opt. Soc. Am. A* **14** 2884 (1997).
7. Liang J, Grimm B, Goels S, Bille J J *J. Opt. Soc. Am. A* **11** 1949 (1994).
8. Haro L D S, Dainty J C *Opt. Lett.* **24** 61 (1999).
9. *American National Standard for the Safe Use of Lasers, ANSI Z136.1* (Orlando FL: Laser Institute of America, 1993).
10. *Normy i pravila ustroystva i ekspluatatsii lazerov* (Rules and Regulations for Laser Devices and Their Operation), No. 5804-91.
11. Born M, Wolf E *Principles of Optics, 4th ed.* (Oxford: Pergamon Press, 1969; Moscow: Nauka, 1973).
12. Koryabin A V, Polezhaev V I, Shmal'gauzen V I *Kvantovaya Electron.* **20** 1031 (1993) [*Quantum Electron.* **23** 899 (1993)].